

# Long-chain branching in slurry polymerization of ethylene with zirconocene dichloride/modified methylaluminoxane

E. Kolodka, W.-J. Wang, P.A. Charpentier, S. Zhu\*, A.E. Hamielec

*Department of Chemical Engineering, McMaster University, Hamilton, Ontario, Canada L8S 4L7*

Received 22 December 1998; received in revised form 12 August 1999; accepted 20 August 1999

## Abstract

We report an experimental investigation on long chain branching (LCB) in ethylene slurry polymerization with bis(cyclopentadienyl) zirconium dichloride ( $\text{Cp}_2\text{ZrCl}_2$ )/modified methylaluminoxane (MMAO) using a semi-batch reactor. The effects of the reaction temperature, pressure, MMAO concentration, and catalyst feeding method on the long chain branching density (LCBD, number of branches per 10 000 carbons), polymer molecular weight, and shear thinning property ( $I_{10}/I_2$ ) were systematically examined. The slurry polymerization process, with its associated polymer-rich phase and the partitioning of active sites, favors the LCB formation via an in situ copolymerization of ethylene macromonomers generated by  $\beta$ -hydride elimination and chain transfer to monomer. Increasing the temperature from 60 to 80°C reduced the LCBD from 0.33 to 0.10, while increasing the pressure from 2 to 20 psig reduced the LCBD from 0.73 to 0.30. The LCB polyethylenes showed enhanced shear thinning properties, with melt flow index ratios ( $I_{10}/I_2$ ) in the range of 8.8–21.5. The feeding sequence of reactants also had a significant effect on the LCB formation. It was observed that feeding ethylene monomer before zirconocene catalyst produced polyethylenes having much higher LCBD than feeding catalyst before monomer. © 2000 Elsevier Science Ltd. All rights reserved.

*Keywords:* Metallocene catalyst; Long-chain branching; Polyethylene

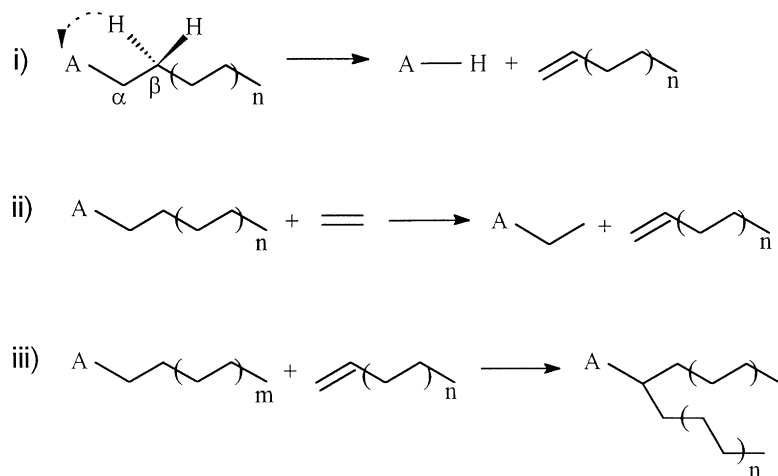
## 1. Introduction

Metallocene polymerizations are poised to revolutionize the polyolefins industry. These catalysts, along with the development of MAO in the early 1980s by Kaminsky and Sinn, offer many advantages over traditional Ziegler–Natta (Z–N) catalysts. Metallocenes are extremely active [1,2], and are single site type catalysts. These single-site type catalysts produce polymers with narrow molecular weight distributions (MWDs) and extremely narrow chemical composition distributions (CCDs). Metallocenes can also be tailored to an almost limitless number of site types for a single monomer type or monomer pair by varying: (a) ligand type, (b) bridge joining ligands, (c) substituents on ligands and bridge to alter the steric and electronic surroundings of the active center, and (d) transition metal type [3]. This combination of specificity enables the production of polymers with tailored properties.

Metallocene polymers, due to their narrow MWDs, normally have higher zero-shear viscosities ( $\eta_0$ ) than conventional Z–N resins with the same weight-average

molecular weights ( $M_w$ ). This higher  $\eta_0$  leads to improved mechanical and physical properties, such as enhanced toughness. The narrow MWDs of metallocene polymers, however, induce difficulties in processing (i.e. extrusion, injection molding, etc.) due to a significant lack of shear thinning. The effects of long chain branching (LCB) on the mechanical and rheological properties of polymers are known to be quite remarkable [4,5]. LCB polyethylene (PE) with a narrow MWD provides an excellent combination of high mechanical strength and good processibility [6,7]. However, it is difficult to synthesize LCB high-density polyethylenes by ethylene homopolymerization using conventional Z–N catalysts. The recent advent of the constrained geometry catalyst (CGC) has offered a great opportunity for producing LCB polyethylenes [7]. The ‘open’ geometry structure of the CGC allows the addition of high  $\alpha$ -olefins and macromonomers. Scheme 1 (Illustration showing how LCBs are formed by: (i) formation of a macromonomer by  $\beta$ -hydride elimination; (ii) formation of a macromonomer by chain transfer to monomer; and (iii) incorporation of the macromonomer into a growing polymer chain) illustrates the LCB formation: a growing chain is terminated by  $\beta$ -hydride elimination or chain transfer to monomer generating a macromonomer with terminal unsaturation, the macromonomer is

\* Corresponding author. Tel.: +1-905-525-9140; fax: +1-905-521-1350.  
E-mail address: zhuship@mcmaster.ca (S. Zhu).



Scheme 1.

then added to a growing polymer chain to form a branched chain.

Our previous works on ethylene solution homopolymerization [8] and ethylene/octene-1 copolymerization [9] in a high-temperature, high-pressure continuous stirred tank reactor (CSTR) using the CGC, showed that LCB formation most likely proceeded via a reaction of macro-monomer at the same active site. This in situ mechanism illustrates the probability of producing LCB polyethylene by a slurry process. In this paper we have selected bis(cyclopentadienyl) zirconium dichloride ( $\text{Cp}_2\text{ZrCl}_2$ ) for the ethylene slurry polymerization in a semi-batch process. The effects of temperature, pressure, co-catalyst concentration, and reactant feeding method on the LCB, molecular weight and melt flow index (MFI) were examined.

## 2. Experimental

### 2.1. Materials

All manipulations involving air and moisture sensitive compounds were carried out under dry nitrogen in a glove box. The catalyst  $\text{Cp}_2\text{ZrCl}_2$  was purchased from Aldrich and modified methylaluminoxane (MMAO, 12 mol% of isobutylaluminoxane) was provided by Akzo as a 10 wt% solution in toluene. The catalyst and co-catalyst were used without further purification. Reagent grade toluene, provided by Caledon Laboratories, was refluxed over metallic sodium/benzophenone for 48 h, and was distilled under a nitrogen atmosphere prior to use. Ethylene (polymerization grade >99.5%) was provided by Matheson Gas and further purified by passing through columns with CuO (Aldrich),

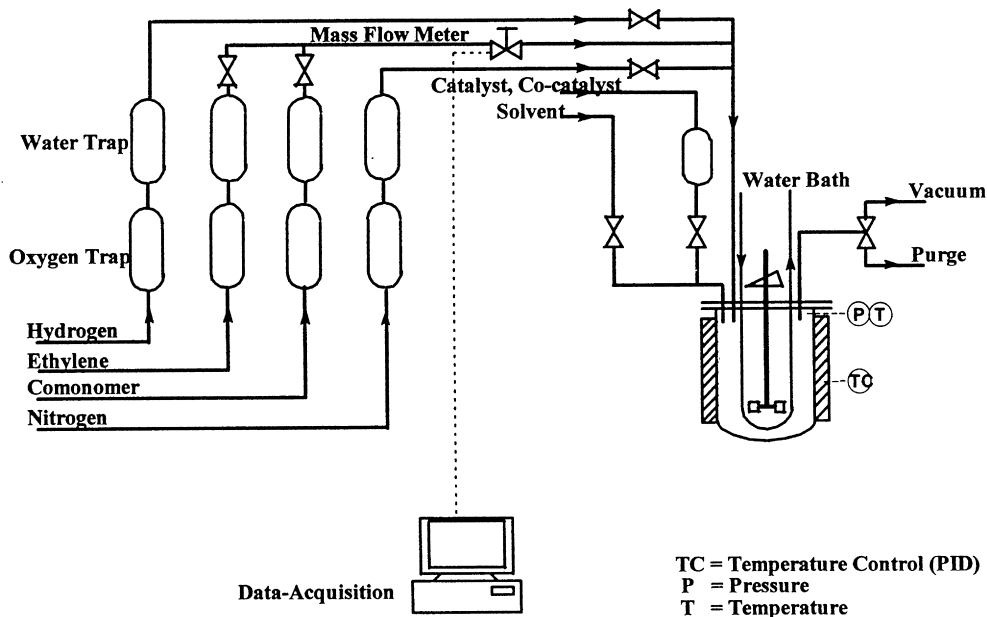


Fig. 1. Schematic of the semi-batch reactor system.

Table 1

Experimental conditions for ethylene homopolymerization using metallocene catalyst systems (polymerization conditions were: catalyst =  $\text{Cp}_2\text{ZrCl}_2$ , co-catalyst = MMAO, solvent = toluene, solvent volume = 700 ml. SB = semi-batch reactor,  $\tau$  = residence time for continuous reactor, CSTR = continuous stirred tank reactor)

Run	Reaction type	Temperature ( $^{\circ}\text{C}$ )	Pressure (psig)	(Catalyst) ( $\mu\text{m}$ )	(Co-catalyst)/(catalyst)	$\tau$ (min)
1	SB	60	10	6.5	1600	–
2	SB	70	10	6.5	1600	–
3	SB	80	10	6.5	1600	–
4	SB	70	2	6.5	1600	–
5	SB	70	5	6.5	1600	–
6	SB	70	20	6.5	1600	–
7	SB	70	10	6.5	800	–
8	SB	70	10	6.5	2400	–
9	Altered SB	70	10	6.5	1600	–
10	Altered SB	80	10	6.5	1600	–
11	Altered SB	70	5	6.5	1600	–
12 [13]	CSTR <sup>a</sup>	140	1500	2	1000	5
13 [8]	CSTR <sup>b</sup>	140	500	15	3	4

<sup>a</sup> Catalyst =  $\text{Cp}_2\text{ZrCl}_2$ , co-catalyst—MMAO, solvent—toluene, ethylene flow rate = 7.7 g/min.

<sup>b</sup> Catalyst = the Dow Chemical's CGC-Ti, co-catalyst = tris(pentafluorophenyl)boron, 2nd co-catalyst—MMAO at 150  $\mu\text{m}$ , solvent = Isopar-F, ethylene flow rate—6.0 g/min, and hydrogen concentration =  $8.01 \times 10^{-4}$  M.

Ascarite (Fisher Scientific) and molecular sieves (Grace-Davidson) to remove oxygen, carbon dioxide and moisture, respectively.

## 2.2. Polymerization procedure

Polymerization reactions were performed in our 1 l semi-

batch reactor. Fig. 1 shows a flow sheet of the semi-batch system.

All experiments were performed at 1200 rpm, with toluene as the diluent, and with a catalyst concentration of 6.5  $\mu\text{m}$ . A measured amount of diluent was transferred into the nitrogen purged reactor with subsequent purging with nitrogen. The co-catalyst solution was injected by syringe into the reactor. After 5 min the catalyst solution was

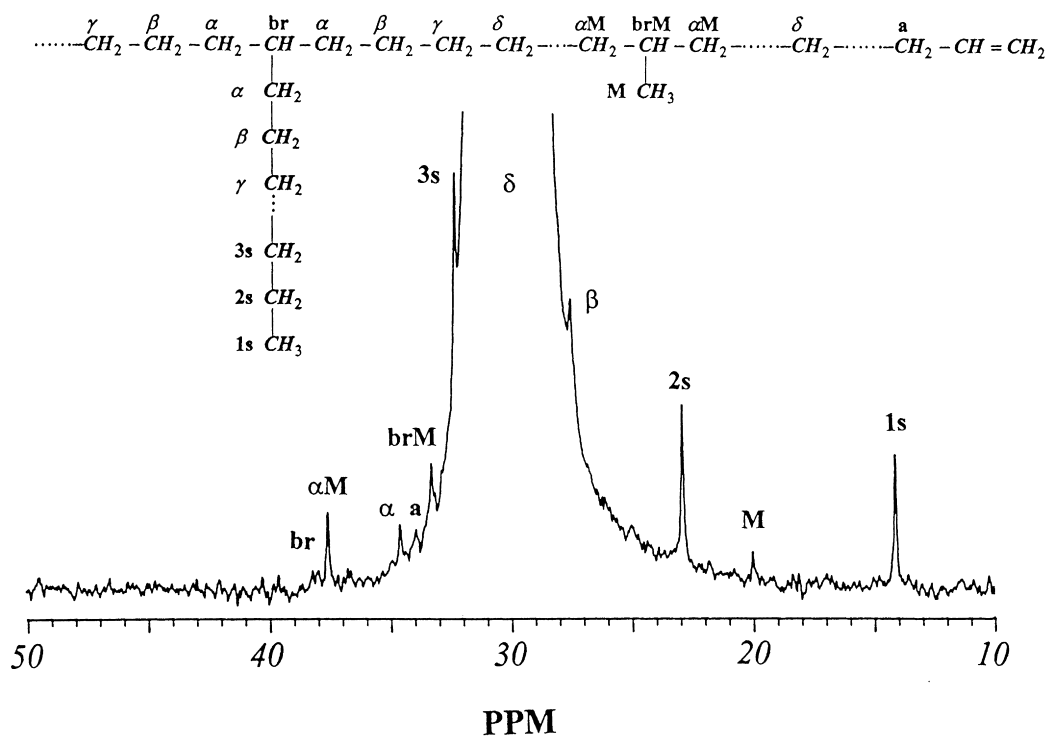


Fig. 2.  $^{13}\text{C}$  NMR spectrum with chemical shifts in TCB and d-ODCB at  $120^{\circ}\text{C}$  for a semi-batch produced PE sample (run 4). The polymerization conditions were:  $[\text{Cp}_2\text{ZrCl}_2] = 6.5 \mu\text{m}$ ,  $[\text{MMAO}]/[\text{Cp}_2\text{ZrCl}_2] = 1600$ ,  $T = 70^{\circ}\text{C}$ ,  $P = 2$  psig.

Table 2  
Summary of GPC,  $^{13}\text{C}$  NMR, and MFI data

Run	$M_w (\times 10^5)$	$M_w/M_n$	LCBD ( $\times 10^4$ )	SCBD ( $\times 10^4$ )	UCED ( $\times 10^4$ )	LCBF	$I_2$	$I_{10}/I_2$
1	2.80	2.44	0.25	0.63	0.76	0.16	–	–
2	1.54	2.54	0.33	1.59	0.74	0.12	0.04	21.5
3	1.08	2.34	0.10	1.03	0.79	0.03	0.70	8.8
4	0.95	2.44	0.73	1.66	1.23	0.22	0.22	17.6
5	1.22	2.63	0.65	1.16	1.06	0.21	0.17	15.5
2	1.54	2.54	0.33	1.59	0.74	0.12	0.04	21.5
6	1.97	2.66	0.30	0.93	0.71	0.15	0.03	21.3
7	1.60	2.40	0.35	0.81	0.89	0.17	0.07	14.8
2	1.54	2.54	0.33	1.59	0.74	0.12	0.04	21.5
8	1.52	2.81	0.21	2.21	0.43	0.07	0.18	13.0
9	0.63	2.15	1.00	1.77	0.89	0.20	2.33	12.9
10	0.57	2.05	0.86	1.94	0.89	0.17	4.20	12.4
11	0.73	2.69	1.01	1.50	0.92	0.21	1.59	11.5
12 [15]	0.33	2.55	0	3.10	4.67	0	29.0	5.64
13 [8]	1.04	2.04	0.35	0	0.65	0.11	0.21	17.8

injected. The polymerization was initiated by the addition of ethylene to the reactor. This procedure was used for all reactions except for those otherwise noted. The reaction was terminated by depressurizing and purging the reactor with nitrogen. The formed polyethylene was washed with methanol to remove MMAO residue, filtered, and dried in a vacuum oven. The detailed polymerization conditions are summarized in Table 1.

### 2.3. Polymer characterization

Molecular weight ( $M_w$ ) and MWD of the polymers were measured using a Waters–Millipore 150 C High Temperature GPC with a differential reflective index (DRI) detector. The polymer samples were dissolved in 1,2,4-trichlorobenzene (TCB) at a concentration of 0.1 wt% and measured at 140°C with a flow rate of 1 ml/min. The GPC was equipped with three linear mixed Shodex AT806MS columns. The retention times were calibrated at 140°C against known monodisperse TSK polystyrene (PS) standards from TOYO SODA Mfg. Co. The Mark–Houwink constants for the universal calibration curve were  $K = 2.32 \times 10^{-4}$  and  $\alpha = 0.653$  for PS and  $K = 3.95 \times 10^{-4}$  and  $\alpha = 0.726$  for PE.

$^{13}\text{C}$  NMR spectra were acquired on a Bruker AC 300 pulsed NMR spectrometer operated at 75.4 MHz with broad band decoupling. The samples were dissolved in deuterated *o*-dichlorobenzene (d-ODCB) and TCB, and were measured at 120°C using 10-mm sample tubes. d-ODCB was used to provide an internal lock signal, and TCB was the internal reference. Spectra required more than 7000 scans to attain an acceptable signal-to-noise ratio. A repetition time of 10 s was utilized [8].

Fig. 2 gives a spectrum of a polyethylene sample produced in this work (run 4). The chemical shifts assigned to different carbonyl groups followed the references [10–12]. The long chain branching density (LCBD, the number of branching points per 10 000 carbons), short chain

branching density (SCBD, the number of branching points per 10 000 carbons), unsaturated chain end density (UCED, the number of unsaturated chain ends per 10 000 carbons), and long chain branching frequency (LCBF, the number of long chain branch points per polymer molecule) were calculated using the equations

$$\text{LCBD} = \frac{\text{IA}_\alpha}{3\text{IA}_{\text{Tot}}} \times 10\,000 \quad (1)$$

$$\text{SCBD} = \frac{\text{IA}_{\alpha\text{M}}}{2\text{IA}_{\text{Tot}}} \times 10\,000 \quad (2)$$

$$\text{UCBD} = \frac{\text{IA}_\alpha}{\text{IA}_{\text{Tot}}} \times 10\,000 \quad (3)$$

$$\text{LCBF} = \frac{2\text{LCBD}}{\text{SCBD} + \text{UCBD} - \text{LCBD}} \quad (4)$$

where the saturated chain end density  $\text{SCED} = (\text{IA}_{1\text{s}} + \text{IA}_{2\text{s}})/2\text{IA}_{\text{Tot}} \times 10\,000$ ;  $\text{IA}_\alpha$ ,  $\text{IA}_{\alpha\text{M}}$ ,  $\text{IA}_{1\text{s}}$ ,  $\text{IA}_{2\text{s}}$ ,  $\text{IA}_a$ , and  $\text{IA}_{\text{Tot}}$  are the integral areas of  $\alpha$ -CH<sub>2</sub>,  $\alpha$ M-CH<sub>2</sub>, 1s, 2s, a-CH<sub>2</sub>, and total intensity of carbons, respectively. In integrating the resonance peaks close to the peak  $\delta^+$ , the baseline effect by the “tree trunk” of peak  $\delta^+$  was subtracted from the signals.

Melt flow indexes were determined with a Kayeness Melt Flow Indexer at 190°C according to the ASTM D-1238 method. The test loads for  $I_2$  and  $I_{10}$  were 2.16 and 10 kg, respectively. Polyethylene samples were prepared by mixing 0.6 wt% Irganox 1010 (an antioxidant) in acetone, adding PE, followed by subsequent drying in a vacuum oven. The polymer samples were typically white.

## 3. Results and discussion

### 3.1. Long chain branching in slurry polymerization

Table 2 summarizes the high temperature GPC,  $^{13}\text{C}$

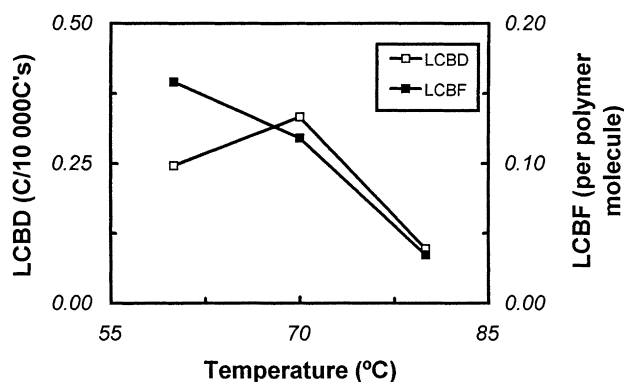


Fig. 3. The effect of temperature on LCB density and frequency. The polymerization conditions were:  $[\text{Cp}_2\text{ZrCl}_2] = 6.5 \mu\text{m}$ ,  $[\text{MMAO}]/[\text{Cp}_2\text{ZrCl}_2] = 1600$ ,  $P = 10$  psig.

NMR, and MFI characterization results. Also included in this table is a PE sample produced in a high temperature, high pressure continuous stirred-tank reactor (CSTR) with toluene as the diluent using the same catalyst system [13]. The CSTR reaction temperature was higher than the melting point of PE, ensuring a homogeneous system with no polymer precipitation. Homogeneous polymerization at high temperature is believed to increase the diffusion of the polymer chains, hence making ethylene macromonomers more mobile and reactive. However, no LCB was observed in the polymer sample produced by the CSTR using  $\text{Cp}_2\text{ZrCl}_2$  with only short chain branching present owing to chain isomerization [8,14,15]. In comparison,  $^{13}\text{C}$  NMR spectra of PE samples produced in the slurry polymerization (Fig. 2) clearly show the presence of LCB structures. This indicates that the slurry polymerization enhances LCB formation using  $\text{Cp}_2\text{ZrCl}_2$ .

During the slurry polymerization, the catalyst and co-catalyst interact to form cationic active sites, which polymerize ethylene monomer to form polymer chains. The polymer chains, due to poor solubility at low reaction temperatures [16,17], are believed to precipitate out of solution upon formation and encapsulate the active centers. The precipitated polymers, swollen with solvent, form a polymer rich phase. Ethylene diffuses into this polymer-rich phase and propagates. While the ethylene propagation reaction proceeds,  $\beta$ -hydride elimination and/or transfer to monomer occur to form ethylene macromonomers (see Scheme 1). These macromonomers are “frozen” in the polymer-rich phase and trapped in close proximity to the active centers, allowing further reactions at the same active site to form LCBs. Moreover, the formation of long chain branches depends on the competing reactions between monomer propagation and macromonomer insertion. The great ratio of macromonomer to monomer within the polymer rich phase facilitates the LCB formation.

LCB polyethylenes were also synthesized by chromium [18], vanadium [19], and palladium-based catalyst [20], as well as some metallocenes such as  $\text{Et}[\text{Ind}]_2\text{ZrCl}_2$  and

$\text{Et}[\text{IndH}_4]_2\text{ZrCl}_2$  in slurry and gas-phase polymerizations [21,22]. Three mechanisms were proposed to explain the long chain branching in ethylene/catalyst systems: (1) copolymerization of ethylene with ethylene macromonomer generated in situ via  $\beta$ -hydride elimination and/or transfer to ethylene [8]; (2) chain walking followed by ethylene insertion [20]; (3) intermolecular C–H bond activation through  $\sigma$ -bond metathesis reaction [19]. Which of the mechanisms is actually involved in branching depends on the catalyst type and experimental conditions. Since there was no LCB observed in our solution ethylene polymerization experiments using the same catalyst system [13], we believe that the branching mechanism involved in this work is via the ethylene macromonomer copolymerization.

The LCB polyethylenes showed enhanced shear thinning properties. The melt flow index ratios  $I_{10}/I_2$  were in the range of 8.8–21.5 as shown in Table 2. It should be pointed out that the shear-thinning behavior of a polymer is determined by many chain parameters, including molecular weight, molecular weight distribution, long chain branching density, and branch chain length. Although an increase in the  $I_{10}/I_2$  with LCB can be clearly seen in Table 2 (data with the same reactor type), a comprehensive relationship between the chain structure and polymer shear thinning is yet to be developed.

$^{13}\text{C}$  NMR determination also indicates the existence of methyl side groups in the PE samples. It is believed that this is due to a same-site 2-1 insertion of ethylene macromonomer immediately after  $\beta$ -hydride elimination. This phenomenon was also observed in the continuous solution polymerization of ethylene at temperatures over  $180^\circ\text{C}$  using the CGC system [8].

Compare the sample of semi-batch run 4 (LCBD 0.73,  $M_w$   $0.95 \times 10^5$  and MWD 2.44) to the CSTR CGC-PE (LCBD 0.35,  $M_w$   $1.04 \times 10^5$ , and MWD 2.04). The melt flow indexes ( $I_2$  and  $I_{10}/I_2$ ) for both samples are very similar (run 4 sample:  $I_2 = 0.22$  and  $I_{10}/I_2 = 17.6$ ; CGC-PE:  $I_2 = 0.21$  and  $I_{10}/I_2 = 17.8$ ). However, these polymers have a large difference in LCBD. This may indicate that the branches generated in the CGC solution polymerization have longer chain lengths and induce higher shear sensitivities than those in the  $\text{Cp}_2\text{ZrCl}_2$  slurry process.

### 3.2. Effect of polymerization temperature

The temperatures studied were 60, 70 and  $80^\circ\text{C}$  (runs 1–3). Fig. 3 shows the effect of temperature on the LCB density and frequency. Increasing the temperature from 60 to  $80^\circ\text{C}$  significantly reduced the polymer molecular weight and LCBF. However, temperature had a minor effect on the level of residual unsaturated chain ends. The effect of temperature on LCB can be explained by the solubility of the polymer chains [16,17]. At higher temperatures, more polymer chains are dissolved in solvent and there is consequently a smaller polymer rich phase. Thus elevating temperature from 70 to  $80^\circ\text{C}$  lowered LCBDs from 0.33

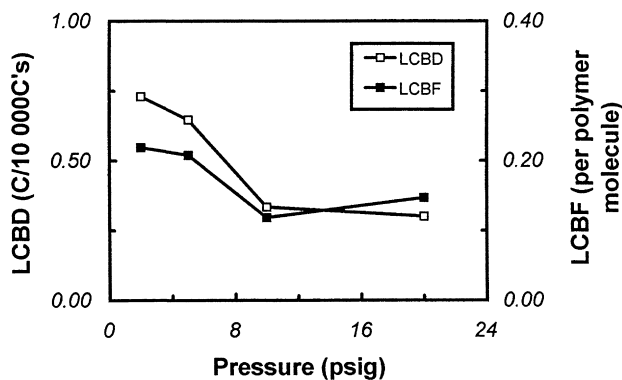


Fig. 4. The effect of pressure on LCB density and frequency. The polymerization conditions were:  $[\text{Cp}_2\text{ZrCl}_2] = 6.5 \mu\text{m}$ ,  $[\text{MMAO}]/[\text{Cp}_2\text{ZrCl}_2] = 1600$ ,  $T = 70^\circ\text{C}$ .

to 0.10. On the contrary, temperature also affects the monomer solubility in solvent [17], and thus influences the concentration ratio of ethylene monomer to macromonomer in the polymer rich phase. Increasing temperature not only decreases the polymer rich phase, but also decreases the ethylene concentration in solvent and in turn the ethylene concentration in the polymer rich phase. These competing factors raised the LCB density from 0.25 to 0.33 for the temperature from 60 to 70°C. The long chain branching frequency, LCBF, is the combination of the polymer molecular weight and LCB density. At lower temperatures the molecular weights were much higher and consequently the LCBF increased. Therefore, the LCBF increased from 0.03 to 0.16 when the temperature decreased from 80 to 60°C.

### 3.3. Effect of polymerization pressure

Four polymerization pressures, 2 (run 4), 5 (run 5) 10 (run 2) and 20 psig (run 6), were investigated in this work. The effect of pressure on the LCB density and LCBF is shown in Fig. 4. The pressure of the polymerization system determines the

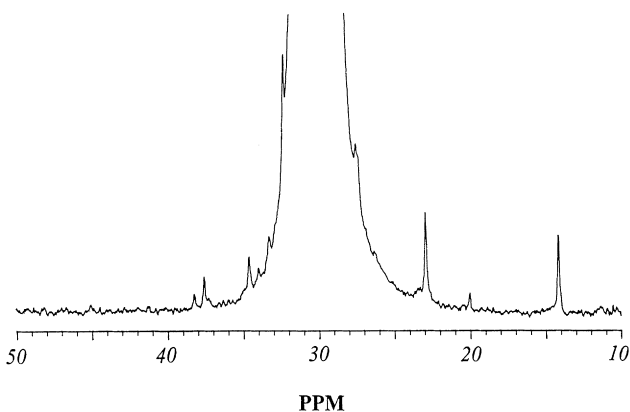


Fig. 5.  $^{13}\text{C}$  NMR spectrum in TCB and d-ODCB at 120°C for a semi-batch produced PE sample (run 9) using the altered procedure. The polymerization conditions were:  $[\text{Cp}_2\text{ZrCl}_2] = 6.5 \mu\text{m}$ ,  $[\text{MMAO}]/[\text{Cp}_2\text{ZrCl}_2] = 1600$ ,  $T = 70^\circ\text{C}$ ,  $P = 10$  psig.

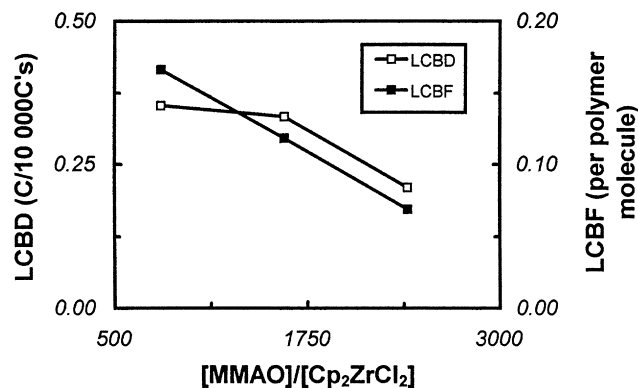


Fig. 6. The effect of  $[\text{MMAO}]/[\text{Cp}_2\text{ZrCl}_2]$  on LCB density and frequency. The polymerization conditions were:  $[\text{Cp}_2\text{ZrCl}_2] = 6.5 \mu\text{m}$ ,  $T = 70^\circ\text{C}$ ,  $P = 10$  psig.

ethylene concentrations in the solvent and polymer rich phases. The formation of ethylene macromonomers depends on the competition between monomer insertion and chain transfer reactions ( $\beta$ -hydride elimination and chain transfer to monomer). Lowering monomer concentration in the polymer rich phase leads to higher unsaturation of polymer chains and thus higher UCED and SCBD. The effect of pressure on the monomer concentrations also influences molecular weight, LCB density and LCBF. Increasing pressure from 2 to 20 psig increased  $M_w$  from 0.95 to  $1.97 \times 10^5$ , while decreased LCB density from 0.73 to 0.30.

### 3.4. Effect of polymerization procedure

The order in which the reactor was charged with reactants had a strong influence on the molecular weight and branching formation of the PE. In the altered procedure the system was saturated with ethylene immediately after the injection of MMAO. The reaction was then initiated by the injection of catalyst five minutes later. Runs 9–11 used this altered procedure and correspond to the experimental conditions in runs 2, 3 and 5, respectively, as shown in Table 2. In all cases, the altered procedure produced polymers with higher LCB density, SCBD, UCED, and with lower molecular weights compared with their analogous runs. A  $^{13}\text{C}$  NMR spectrum of run 9, given in Fig. 5, clearly shows the increase of branching intensities. Because the polymerization system was initially saturated by ethylene, there existed a high monomer concentration at the start of reaction in the altered procedure. When the catalyst was injected into the system it immediately reacted with MMAO to form active sites. Note that the same experimental conditions, excepting the initial monomer concentration in the system, were used in both procedures. It appears that the different experimental results are due to the immediate encapsulation of catalyst and active centers by instantaneous polymer formation in the altered procedure. A larger proportion of active sites was entrapped in the polymer rich phase with significant limitations on monomer diffusion into the active zone. This in turn

served to reduce the MW and enhance LCB formation. This instant encapsulation also affected the morphology of the resultant polymers. PE produced with the standard procedure was composed of fine, uniform particles, while PE formed in the altered procedure was composed of larger, irregular particles.

### 3.5. Effect of MMAO concentration

The effects of the co-catalyst MMAO concentration on the polymer chain structures are shown in Fig. 6 and Table 2. The ratios of MMAO to  $\text{Cp}_2\text{ZrCl}_2$  concentrations of 800 (run 7), 1600 (run 2), and 2400 (run 8) were used in the present work. This concentration ratio had only a minor effect on the molecular weight of the PE samples, but broadened the MWD at higher MMAO concentrations. This effect is attributed to increased chain transfer to MMAO. Chain transfer to MMAO also reduces the formation of terminal double bonds. Therefore, at high MMAO concentrations the UCED was lower, which lowered both LCBD and LCBF and increased  $I_2$ . Elevated MMAO concentrations also increased the rate of 2-1 insertion of ethylene macromonomer and thus the SCBD.

## 4. Conclusions

Significant long chain branching formation was found by  $^{13}\text{C}$  NMR determinations in PE produced using the homogeneous catalyst cyclopentadienyl zirconium dichloride in a semi-batch slurry polymerization, with LCBD (carbons per 10 000 carbons) up to 1.0. A slurry polymerization process is believed responsible for the formation of LCB. Enhanced levels of LCB are attributed to the in situ reaction of ethylene macromonomer and the encapsulation of active centers by precipitated polymer chains. The experimental conditions of reaction temperature, pressure, initial polymer concentration, and MMAO concentration, all affect LCB formation. High initial polymer concentration had a great influence on the long chain branching density, increasing the LCBD in the PE samples. Increasing the temperature from 60 to 80°C reduced the LCBD from 0.33 to 0.10, while increasing the pressure from 2 to 20 psig reduced the LCBD from 0.73 to 0.30. Different MMAO to  $\text{Cp}_2\text{ZrCl}_2$  ratios also influenced the formation of LCB, with LCBDs ranging from 0.21 to 0.35 at ratios of 2400 to 800. The LCBD

polyethylenes showed enhanced shear thinning properties. The melt flow index ratios  $I_{10}/I_2$  were in the range of 8.8–21.5, with an  $I_2$  ranging from less than 0.1–0.701 g/10 min.

## Acknowledgements

The authors greatly appreciate the financial support from the Natural Sciences and Engineering Research Council of Canada (NSERC) for this work.

## References

- [1] Kaminsky W. In: Quirk RP, editor. Transition metal catalyzed polymerization, 4. London: MMI Press, 1983 p. 225.
- [2] Chien JCW, Wang BP. *J Polym Sci, Polym Chem Ed* 1988;26:3089.
- [3] Hamielec AE, Soares JP. *Progr Polym Sci* 1996;21:651.
- [4] Small PA. *Adv Polym Sci* 1975;18:1.
- [5] Santamaria A. *Mater Chem Phys* 1985;12:1.
- [6] Yan D, Wang W-J, Zhu S. *Polymer* 1999;40:1737.
- [7] The Dow Chemical Co., invs.: Lai SY, Wilson JR, Knight GW, Stevens JC, Chum PWS. US 5,272,236, 1993.
- [8] Wang W-J, Yan D, Zhu S, Hamielec AE. *Macromolecules* 1998;31:8677.
- [9] Wang W-J, Kolodka E, Zhu S, Hamielec AE. *J Polym Sci, Polym Chem Ed* 1999;37:2949.
- [10] Randall JC. Polymer sequence determination, carbon-13 NMR method, New York: Academic Press, 1977 p. 95.
- [11] Determination of linear low density polyethylene (LLDPE) composition by carbon- $^{13}$  NMR, ASTM D 5017-91, 1991.
- [12] De Pooter M, Smith PB, Dohrer KK, Bennett KF, Meadows MD, Smith CG, Schouwenaars HP, Geerards RA. *J Appl Polym Sci* 1991;42:399.
- [13] Charpentier PA, Zhu S, Hamielec AE, Brook MA. *Ind Engng Chem Res* 1997;36:5074.
- [14] Johnson LK, Killian CM, Brookhart M. *J Am Chem Soc* 1995;117:6414.
- [15] Deng L, Margl P, Ziegler T. *J Am Chem Soc* 1997;119:1094.
- [16] Orwoll RA. In: Mark HF, Bikales NM, Overberger CG, Menges G, Kroschwitz JI, editors. *Encyclopaedia of polymer science and engineering*, 15. New York: Wiley, 1989. p. 380.
- [17] Gerrard W. *Gas solubilities-widespread applications*, New York: Pergamon Press, 1976.
- [18] Shaffer WKA, Ray WH. *J Appl Polym Sci* 1997;65:1053.
- [19] Reinking MK, Orf G, McFaddin D. *J Polym Sci, Polym Chem Ed* 1998;36:2889.
- [20] Guan Z, Cotts PM, McCord EF, McLain SJ. *Science* 1999;283:2059.
- [21] Malmberg A, Kokko E, Lehmus P, Lofgren B, Seppala JV. *Macromolecules* 1998;31:8448.
- [22] Harrison D, Coulter IM, Wang S, Nistala S, Kuntz BA, Pigeon M, Tian J, Collins S. *J Mol Catal A* 1998;128:65.